Biophysics and Physicobiology

Review Article

High-speed atomic force microscopy imaging of live mammalian cells

Mikihiro Shibata[1,2], Hiroki Watanabe[3], Takayuki Uchihashi[4], Toshio Ando[2] and Ryohei Yasuda[5]

[1]High-speed AFM for Biological Application Unit, Institute for Frontier Science Initiative, Kanazawa University, Kanazawa, Ishikawa 920-1192, Japan
[2]Bio-AFM Frontier Research Center, Kanazawa University, Kanazawa, Ishikawa 920-1192, Japan
[3]Research Institute of Biomolecule Metrology Co., Ltd., Tsukuba, Ibaraki 305-0853, Japan
[4]Department of Physics and Structural Biology Research Center, Graduate School of Science, Nagoya University, Nagoya, Aichi 464-8602, Japan
[5]Max Planck Florida Institute for Neuroscience, Jupiter, Florida 33458, USA

Direct imaging of morphological dynamics of live mammalian cells with nanometer resolution under physiological conditions is highly expected, but yet challenging. High-speed atomic force microscopy (HS-AFM) is a unique technique for capturing biomolecules at work under near physiological conditions. However, application of HS-AFM for imaging of live mammalian cells was hard to be accomplished because of collision between a huge mammalian cell and a cantilever during AFM scanning. Here, we review our recent improvements of HS-AFM for imaging of activities of live mammalian cells without significant damage to the cell. The improvement of an extremely long (~3 µm) AFM tip attached to a cantilever enables us to reduce severe damage to soft mammalian cells. In addition, a combination of HS-AFM with simple fluorescence microscopy allows us to quickly locate the cell in the AFM scanning area. After these improvements, we demonstrate that developed HS-AFM for live mammalian cells is possible to image morpho-genesis of filopodia, membrane ruffles, pits open-close formations, and endocytosis in COS-7, HeLa cells as well as hippocampal neurons.

Key words: Bio-imaging, live-cell imaging, nanotechnology, Probe microscopy, AFM

Corresponding author: Mikihiro Shibata, High-speed AFM for Biological Application Unit, Institute for Frontier Science Initiative, Kanazawa University, Kakuma, Kanazawa, Ishikawa 920-1192, Japan. e-mail: msshibata@staff.kanazawa-u.ac.jp

The possibility of direct visualization of live mammalian cells with high spatiotemporal resolution would provide the advanced knowledge of cellular functions. For example, morphology of synapses of neurons changes dynamically in response to extracellular stimulus and these morphological changes are critical for plasticity and adaptive response of neurons. However, since the size of synapses is only a few hundred nanometers, in order to better understand of the detailed processes of the morphological dynamics of synapses, direct visualization with nanometer resolution under near physiological conditions has long been desired, but remains a challenge.

Atomic force microscopy (AFM) can image a surface topography of objects with nanometer resolution in an aqueous solution and has been used to image a wide variety of

◄ *Significance* ►

Visualization of morphological dynamics of live mammalian cells with nanometer resolution under physiological conditions is highly desired. In this review, we demonstrated that the unprecedented AFM movies show nanometer-scale morphogenesis of filopodia, membrane ruffles, pit formations and endocytosis in living COS-7 and HeLa cells and hippocampal neurons with temporal resolution of seconds. We believe that this method will lead to a great advance in analysis of cellular morphogenesis and have a great impact on a wide range of biological sciences.

biological samples [1–11]. In particular, the appearance of high-speed AFM (HS-AFM), which has been extensively optimized the scanning speed by two orders of magnitudes faster than that of conventional AFM, opened a way to image the conformational change of single molecules on substrates with a subseconds time resolution [12,13]. In the past decade, various dynamic processes of biological samples including photo-induced conformational change of bacteriorhodopsin [14–16], myosin V walking on an actin filament [17] and rotary catalysis of rotorless F_1-ATPase [18], stabilization of membranes by annexin V [19], lipid membrane remodeling by ESCRT-III polymerization [20], reaction processes of DNA targeting enzymes [21], nucleosome dynamics [22,23], local conformational changes of DNA strands [24–27], and dynamics of the nuclear pore complex [28,29], were visualized using HS-AFM. However, applications for nanostructure imaging of live mammalian cells has been complicated, since the length of scale of cells is three orders of magnitude larger than that of proteins. In this review, we introduce three improvements from the original HS-AFM setup to HS-AFM for imaging of live mammalian cells, and demonstrate HS-AFM movies of living COS-7 cells, HeLa cells and cultured hippocampal neurons by 5–10 μm fields at the time resolution of 5–10 seconds per frame, which visualized their cellular activities with nanometer resolution [30].

Development of HS-AFM for imaging of live mammalian cells

To apply HS-AFM for live-cell imaging, three improvements were requried. Frist, we applied a wide-area scanner (photograph is shown in Fig. 1A), which is able to scan about 46×46 μm^2 within 50 seconds per frames [31]. In the mechanical design of a wide-area scanner, we referred the third-class leverage mechanism to amplify the displacements of X- and Y-directions. Specifically, both of the X- and Y-piezoactuators (a nominal unloaded displacement is ~11 μm at 100 V) was symmetrically arranged against the supporting base attached a Z-piezoactuator (a nominal un-

loaded displacement is ~4 μm at 100 V). In this case, the overall lever length is 25 mm. The fulcrum is set at the one end of the lever, while the force point is set as a position of X- or Y-piezoactuator with a length of 5 mm from the fulcrum; i.e., the designed lever ratio is 5. The actual displacements of this designed scanner resulted in ~46.7 μm and ~45.7 μm for the X- and the Y-direction, respectively. A sample stage was glued on the top of a Z-piezoactuator (white arrow in Fig. 1A). In addition, we further improved a wide-area scanner to obtain the best performance for HS-AFM observations, for example, a vibration damping for X-scan, a compensation for nonlinearity, a compensation for interference between X- and Y-scanners and the Z-scanner (Please see the details in our recent review [32]). Using this wide-area scanner, we can image a sample at ~7 second per frame for a scan area of 40×40 μm^2 at 256 pixels^2. The rate-limiting factor for imaging of the cell using a wide-area scanner is determined by the resonant frequency of the Z-piezoactuator (f_R: ~50 kHz). Thus, the X-Y scanning size is enough to image a whole live mammalian cells. Indeed, we demonstrated HS-AFM movies of thin plasma membrane of live HeLa cells in 5×5 μm^2 with temporal resolution of five seconds per frame [31].

Second, a longer AFM tip was applied to avoid collisions between the base of cantilever and living cells. The small cantilever for HS-AFM consists of a bird-beak end with ~1 μm length (Left panel in Fig. 1B). We always fabricated an additional sharp tip on a bird-beak to obtain high-resolution images using electron beam deposition (EBD) by scanning electron microscopy (SEM) [33]. The length of an additional EBD tip used for imaging of biomolecules is less than ~1 μm. However, the tip of this length is unsuited for imaging of live mammalian cells, because the base of cantilever would collide with a taller region of a mammalian cell. To avoid these collisions, we fabricated a longer AFM tip by repeating 1 min EBD for 5–7 times on a bird-beak (the growth rate of an additional EBD tip is ~600 nm per min) [30]. To compensate the mechanical drift of the SEM, the focus position was reset after each EBD cycle. According to
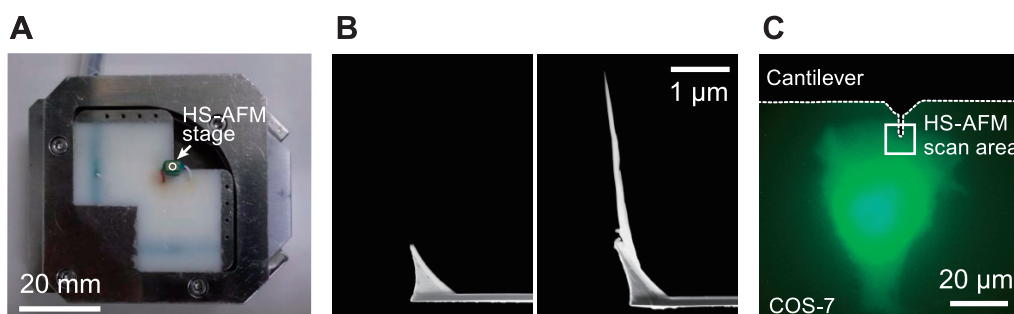

Figure 1　HS-AFM setup for observations of live mammalian cells. (A) Photograph of a wide-area scanner (B) Scanning electron microscopy (SEM) imaging of the end of the cantilever with and without an electron-beam-deposit (EBD) tip. The tip length is about 3 μm for live-cell HS-AFM. (C) Epi-fluorescence images of a COS-7 cell transfected with mEGFP. The white broken lines highlighted the base of a cantilever. The white square indicates a HS-AFM scanning area. HS-AFM images corresponds to Figure 2.

this procedure, the length of a AFM tip for live-mammalian cells optimized about 3 μm, which is almost three times longer than that of the original AFM tip (Right panel in Fig. 1B). While the apex radius of a long AFM tip still has a diameter of less than ~4 nm, which is similar to that of the original AFM tip. This indicate that the sharp and long HS-AFM tip keeps the image quality as nanometer resolution (Fig. 1B).

Third, HS-AFM was combined with simple fluorescence microscope to locate the region of interest of living cells within the AFM scanning area. Even if we use a wide-area scanner for imaging a cell, it is difficult to find a single cell on a HS-AFM stage, because the maximum scanning area of the wide-area scanner is ~46 μm², while the diameter of a HS-AFM stage is ~1.5 mm. Furthermore, a central part of the mammalian cell is easily deformed by the loading force from the AFM tip and, therefore, hard to be imaged. To locate the AFM tip to the flat peripheral region of the cell, simple fluorescence microscopy system was equipped to the standard HS-AFM. The excitation lamp, dichroic filters and a CCD camera are installed under the standard HS-AFM setup. Thus, based on the epi-fluorescence image of GFP expressed living cells, we observed the overall shape of the cell and then located the cell in HS-AFM scanning area (Fig. 1C). In addition, the cantilever was largely oscillated for HS-AFM imaging of live mammalian cells to climb over huge cell protrusions. The free amplitude of HS-AFM imaging for tiny proteins is ~1 nm, while for live mammalian cells is ~100 nm (resonant frequency is ~800 kHz). Thus, improved AFM set up involving the adoption of a wide-area scanner, a manufacturing a longer AFM tip and a combination with epi-fluorescent microscopy, robustly steps over huge live

mammalian cells without significant damages during HS-AFM scanning.

Morphological dynamics of live COS-7 and HeLa cells at the leading-edge

Using developed HS-AFM system, we first observed live-cell lines such as COS-7 and HeLa cells. Figure 1C show the fluorescence image of a mEGFP transfected COS-7 cell. And the corresponding to a sequence of HS-AFM topographical images is shown in Figure 2. At the leading edge of a COS-7 cell, the HS-AFM movie shows constant membrane ruffling and extension or retraction of filopodium for at least 15 min (Fig. 2). We tried to confirm whether these cellular morphologies really relate to cell activities, we applied cytochalasin D, which inhibits actin polymerization [34]. As we expected, after the addition of cytochalasin D, those morphological dynamics at the leading edge observed before gradually abolished (Fig. 2). Subsequently, after washout for ~30 min by the imaging solution, morphological dynamics of COS-7 cells completely recovered, suggesting that membrane dynamics observed by HS-AFM requires actin polymerization.

Interestingly, the addition of some growth factors activates membrane dynamics at the leading edge of cells. After the addition of insulin, which is a hormone as a growth factor of mammalian cells, membrane ruffling became dramatically larger (dashed circles in Fig. 3A). Specifically, a height of the leading edge became taller and the speed of the repeated membrane ruffling was accelerated. Furthermore, some pits appeared on the cell surface, implying that endocytic events frequently occurred by the stimulation of insulin
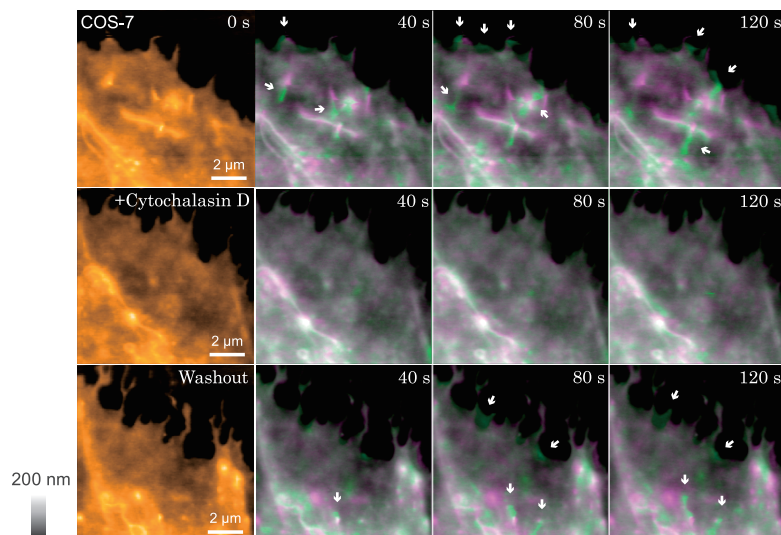

Figure 2 HS-AFM images of a living COS-7 cell. A HS-AFM topographical image acquired from the area indicated in white box in Figure 1C before the addition of cytochalasin D (Top), after application of 20 ng/mL cytochalasin D (middle) and following washout for 30 min (bottom). HS-AFM images taken at the indicated times (green) and the image taken at 0 s (magenta) are overlaid. White arrows indicate newly appeared structures at the leading edge. HS-AFM imaging rates, 10 second per frame. HS-AFM pixel resolutions, 200×200 pixels².
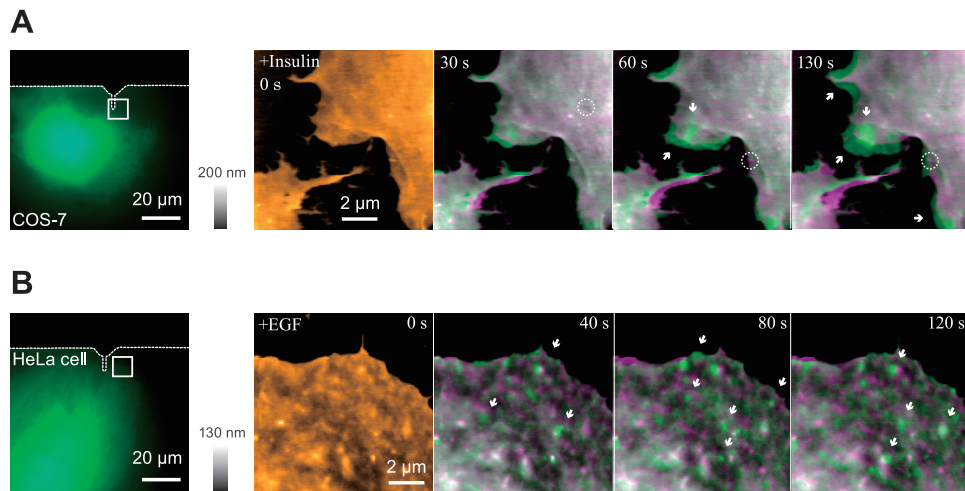
Figure 3 HS-AFM images of living COS-7 and HeLa cells in response to extracellular stimuli. (A) Fluorescence image of a COS-7 cell trans-fected with mEGFP. The white square corresponds to the HS-AFM scanning area. A HS-AFM topographical image acquired after application of 20 mg/mL insulin. HS-AFM images taken at the indicated times (green) and the image taken at 0 s (magenta) are overlaid. Before the addition of insulin, cells were starved with serum-free medium at least for 1 hour. White arrows indicate newly appeared structures. Dashed circles indicate the pits formation. (B) Fluorescence image of a HeLa cell transfected with mEGFP. The white square corresponds to the HS-AFM scanning area. A HS-AFM topographical image acquired after application of 20 ng/mL EGF. HS-AFM images taken at the indicated times (green) and the image taken at 0 s (magenta) are overlaid. Before the addition of EGF, cells were starved with serum-free medium at least for 1 hour. White arrows indicate accelerated surface flow on cell surface. HS-AFM imaging rates, 10 second per frame. HS-AFM pixel resolutions, 200×200 pixels^2.

(Fig. 3A). In addition, the response to the external stimulus was also observed on HeLa cells by the addition of epi-dermal growth factor (EGF). In HeLa cells, HS-AFM movie showed that there is a flow caused by actin polymerization on the cell surface [31]. The direction of this flow is constant from the leading edge to the cell center (Fig. 3B). After the addition of EGF, the flow speed of surface membrane was accelerated dramatically (Fig. 3B). Thus, HS-AFM observa-tions of the leading edge of living cells directly visualized morphological dynamics, which originate from actin polym-erization.

Endocytosis of live COS-7 cells on the cell surface

We next observed the membrane dynamics at the center of live mammalian cells, where is closed to the nucleus (Fig. 4A). At the center of COS-7 cells, there is no unidirectional flow on the membrane surface. Instead, HS-AFM movie shows growths of protrusions in a vertical direction on the membrane surface and the appearance of the soft structure from the inside of the cell. In addition, many pits were observed on the membrane surface, and they constantly repeated the open and close forms on a specific area. In Fig-ure 4B shows that time courses of the depth and height of the pits (Fig. 4B). To confirm pits formations are related to the cell activity, we applied a pharmacological experiment during HS-AFM observations. After the application of dyna-sore, which is an inhibitor of dynamin, pits formations were disappeared (Fig. 4C). Subsequently, formations of pits were recovered by washing out the drug for ~30 min by the imag-

ing solution, suggesting that the observed pits on the cell surface are related to dynamin dependent endocytosis (Fig. 4C). When we overexpressed the constitutive active mutant of Rab5 [Rab5(Q79L)], which positively regulates endo-cytosis, HS-AFM movies of a COS-7 cells transfected with Rab5 mutant clearly shows that the frequency of pits forma-tion increased, and the lifetime of pit was shorter than that of a COS-7 cell transfected with mEGFP (Fig. 4D, E). Thus, those results suggest that the observed pits on the cell sur-face are tightly associated with endocytosis. Interestingly, when pits closed, we often observed "cap-type" endocytosis, in which pits are closed with protrusions formed near the pits (Fig. 4B and Fig. 5). The height analysis in Figure 4B clearly shows the formation of the protrusion just after a pit closed (Fig. 4B). We hypothesize that a biological meaning of "cap-type" endocytosis is to gain the efficiency of a nutrient ingestion by once endocytosis, as if a protrusion cap is a scoop net. We noted that this "cap-type" endocytosis was also observed in COS-7, HeLa cells, as well as hippocampal neurons, implying the common endocytosis mechanism of mammalian cells (Fig. 8C). Moreover, pits repeatedly appeared on the specific area implying the existence of an endocytic "hot spot" on the cell surface (Fig. 4E).

Morphological dynamics of live neurons

From the above, the developed HS-AFM imaging of live mammalian cells could be performed for more than 30 min without any obvious damage to the cell. Using this HS-AFM, we next applied to directly visualize morphological dynam-
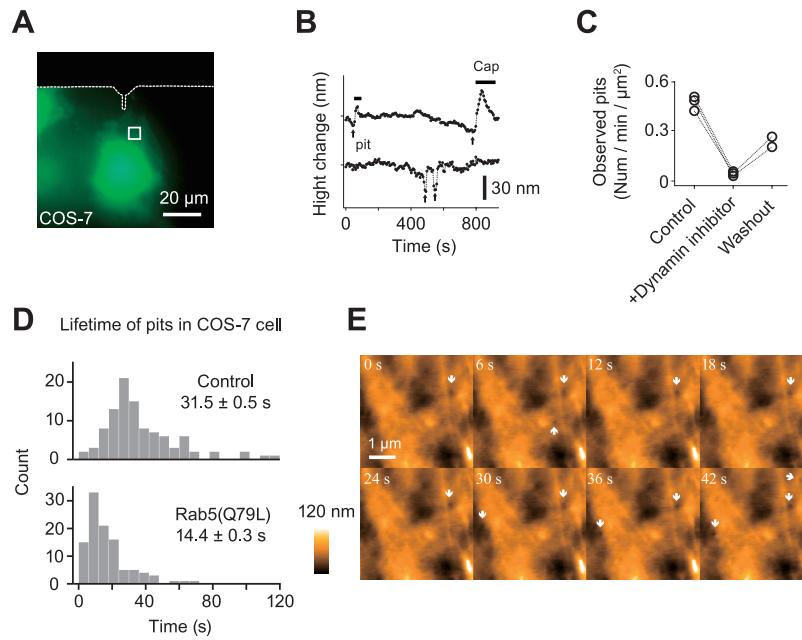
Figure 4   Pits formation on the plasma membrane of a living COS-7 cell. (A) Fluorescence images of a COS-7 cells transfected with mEGFP. The area indicated with the white square was subjected to HS-AFM imaging. (B) Time courses of the depth of pits with and without closure caps. Bars indicate the formation of closure caps. Arrows indicate pit formation. (C) The number of observed pits per min per μm^2 area before, after and washout of dynasore application. (D) The histogram of the lifetime of pits for COS-7 cells transfected with mEGFP (control, upper) and mEGFP-Rab5(Q79L) (bottom). The number of total analyzed pits are 101 and 106 for COS-7 cells transfected with mEGFP and mEGFP-Rab5(Q79L), respectively (3 cells each). (E) A sequence of HS-AFM topographical images of a COS-7 cell transfected with constitutively active Rab5 mutant [mEGFP-Rab5(Q79L)]. The white arrows indicate pits formations. HS-AFM imaging rates, 6 second per frame. HS-AFM pixel resolutions, 200×200 pixels^2.
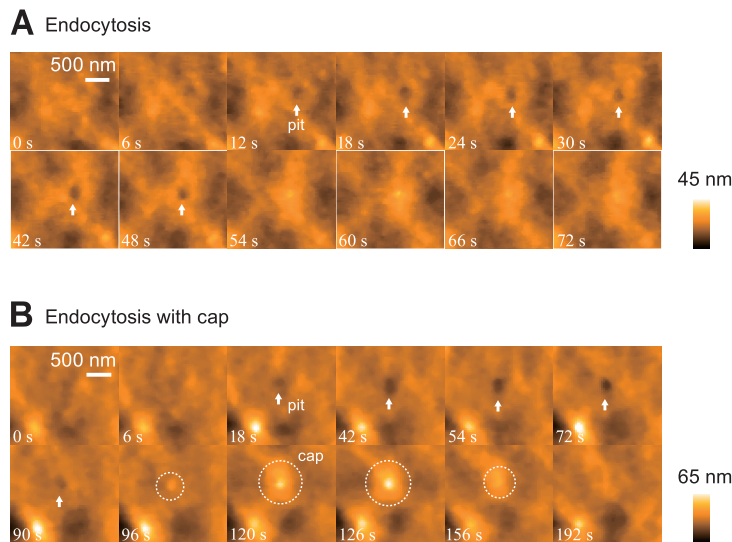

Figure 5   HS-AFM images of endocytosis on the plasma membrane. (A, B) A sequence of magnified HS-AFM images of a living COS-7 cell transfected with mEGFP, taken at 6 seconds per frame, during the pit formation and the closure of the pit with a cap. Arrows indicate the formation of the pit. Dotted circles indicate the formation of the closure cap.

ics of living neurons. On the other hand, we first required to optimize a culture method of neurons. After a process of many trials and errors for improving culturing methods for hippocampal neurons [35–38], we found that low-density dissociated-cell cultures of hippocampal neurons from rats co-cultured with glia cells was the most suitable methods for HS-AFM observations. Figure 6 shows the Scanning Electron Microscopy (SEM) imaging of cultured hippocampal
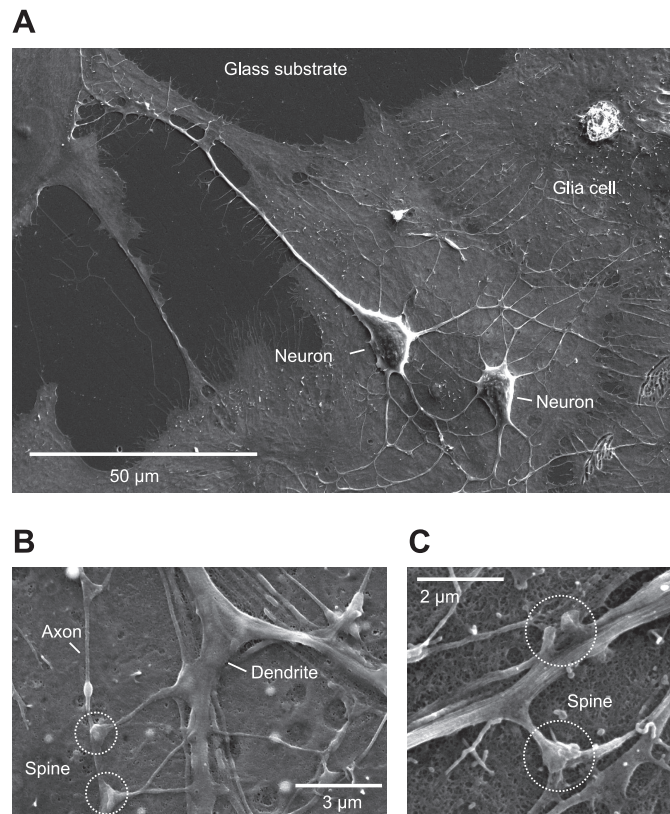
A

B   **C**

Figure 6   SEM imaging of fixed cultured hippocampal neurons. (A) Overall images of cultured hippocampal neurons at 2 days in vitro. (B, C) SEM imaging of cultured hippocampal neurons at 21 days in vitro.

neurons at 2 (Fig. 6A) and 21 (Fig. 6B, C) days in vitro (DIV). Using co-cultured with glia cells methods, neurons survived for 3 weeks even though spines grew on dendrites (Fig. 6B, C).

Figure 7 shows fluorescence imaging of mEGFP transfected cultured hippocampal neurons and corresponding to a sequence of HS-AFM topographical images at 9 DIV (Fig. 7). In 9 DIV, HS-AFM movie shows the extension and retraction of a filopodia. The filopodia grew toward everywhere with several branches, then finally moved back to the original shape after ~20 min (Fig. 7B). Also, Figure 8 shows the HS-AFM imaging of live hippocampal neurons at 13 DIV. The sequence of HS-AFM image shows two different dendritic structures. The central part is tall and rigid structure and is ~1300 nm wide and ~400 nm high (Fig. 8B). As surrounding the rigid structure, the flat and dynamic structure was observed. This dynamic structure is ~150–500 nm wide and ~70 nm high, and showed membrane ruffling like the leading edge of COS-7 cells. In addition, pits appeared on the dendrite, suggesting that HS-AFM can observe endocytosis even though on the membrane surface of living neurons (Fig. 8C, D).

In 15 DIV, it is known that cultured hippocampal neurons may have small protrusions on dendrites called spine. The HS-AFM movie shows dynamics of the dendrite and the thin structure belonged to the dendrite. Interestingly, this thin structure shows a quite flexible and change its morphology over a few minutes (Fig. 9B). The rigid structure is 1500–2000 nm wide and ~590 nm high, while the thin flexible structure is ~140 nm high with different shapes. We note that those kinds of dynamics of the growth of filopodia at 9 DIV, the dendritic membrane ruffling at 13 DIV and the dynamics of small protrusion at 15 DIV were observed only living neurons on glia cells. This fact strongly suggests the importance of physical contacts between neurons and glia cells for their dynamic morphological changes.

Conclusions

The optimization of HS-AFM for live-cell imaging provides direct visualizations of morphological dynamics of live mammalian cells. Especially, the success of HS-AFM observations of living neurons would make possible to directly visualize the morphology dynamics of both pre- and postsynapses during their functions in the near future. After further improvements of HS-AFM techniques, such as combined with fluorescence resonance energy transfer (FRET) imaging or optical nanoscopy techniques [37–40], could add further information about conformational changes of specific receptors by external stimuli on membranes in living neurons.
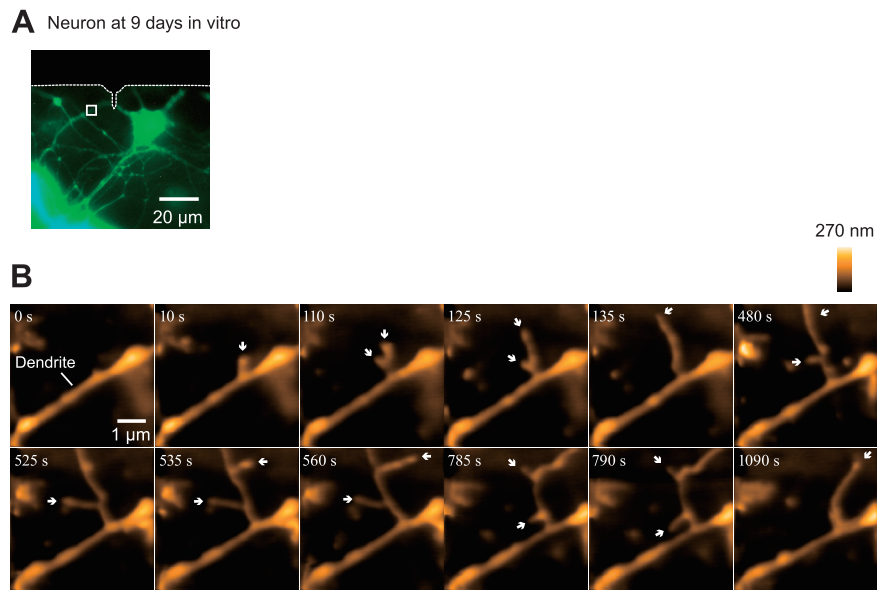
Figure 7 HS-AFM images of a living cultured hippocampal neuron at 9 days in vitro. (A) Fluorescence image of a hippocampal neuron transfected with mEGFP. The white square indicates the HS-AFM scanning area. (B) A sequence of HS-AFM images of a dendrite. The white arrows indicate the growth of dendrite. HS-AFM imaging rates, 5 second per frame. HS-AFM pixel resolutions, 200×200 pixels^2.
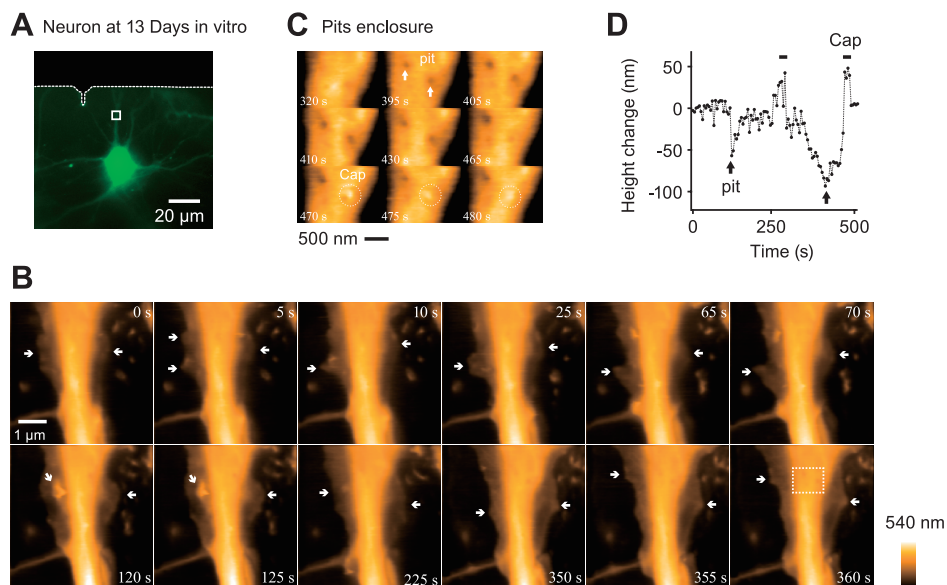

Figure 8 HS-AFM images of a living cultured hippocampal neuron at 13 days in vitro. (A) Fluorescence image of a hippocampal neuron transfected with mEGFP. (B) A sequence of HS-AFM images at 5 s per frame. White arrows indicate the thin, sheet-like ruffling structure. White dotted box at 360 s indicates the magnified region shown in C. (C) A sequence of magnified HS-AFM images during the pits opening and clouser. White arrows indicate the pit formation and dotted red circles indicate the closure cap. (D) Time course of the depth and height of the pit with and without the closure cap. Bars indicate the formation of the closure cap. Arrows indicate pit formations. HS-AFM imaging rates, 5 second per frame. HS-AFM pixel resolutions, 200×200 pixels^2.

Notations

Please see HS-AFM movies of live mammalian cells in the reference No. 30.

Acknowledgements

A Neuron at 15 Days in vitro
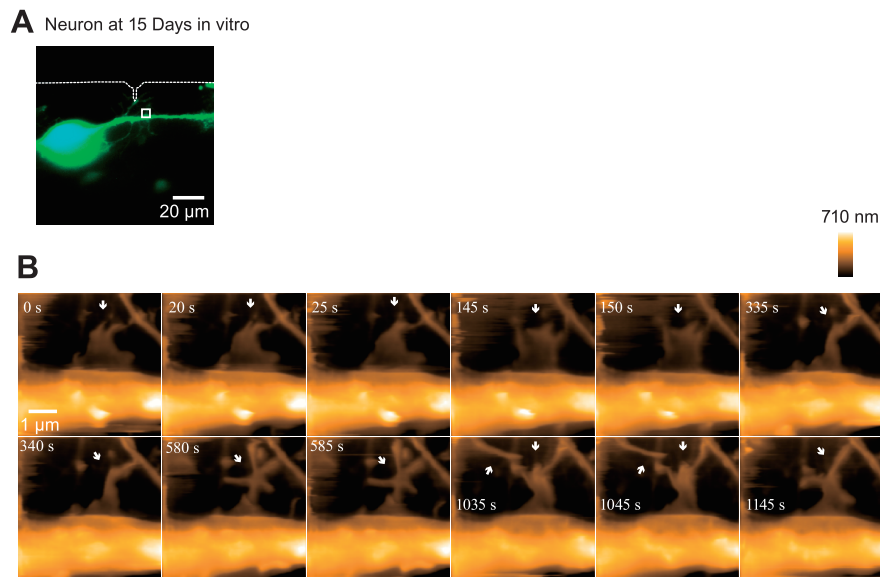
B

710 nm

Figure 9   HS-AFM images of a living cultured hippocampal neuron at 15 days in vitro. (A) Fluorescence image of a hippocampal neuron transfected with mEGFP. Corresponding HS-AFM images for A is shown in B. (B) A sequential HS-AFM topographical images are taken at 5 s per frame. White arrows indicate the dynamics of spine-like structure. HS-AFM imaging rates, 5 second per frame. HS-AFM resolutions, 200×200 pixels^2.

Conflicts of Interest

All the authors declare that they have no conflicts of interest.

Author Contribution

M. S. wrote the manuscript. H. W., T. U., T. A and R. Y. reviewed the manuscript and approved the final form.

References

[1] Binnig, G., Quate, C. F. & Gerber, C. Atomic force microscope. *Phys. Rev. Lett.* **56**, 930–933 (1986).

[2] Dague, E., Alsteens, D., Latge, J. P., Verbelen, C., Raze, D., Baulard, A. R., *et al.* Chemical force microscopy of single live cells. *Nano Lett.* **7**, 3026–3030 (2007).

[3] Hansma, P. K., Elings, V. B., Marti, O. & Bracker, C. E. Scanning tunneling microscopy and atomic force microscopy: application to biology and technology. *Science* **242**, 209–216 (1988).

[4] Henderson, E., Haydon, P. G. & Sakaguchi, D. S. Actin filament dynamics in living glial cells imaged by atomic force microscopy. *Science* **257**, 1944–1946 (1992).

[5] Leuba, S. H. & Bustamante, C. Analysis of chromatin by scanning force microscopy. *Methods Mol. Biol.* **119**, 143–160 (1999).

[6] Mingeot-Leclercq, M. P., Deleu, M., Brasseur, R. & Dufrene, Y. F. Atomic force microscopy of supported lipid bilayers. *Nat. Protoc.* **3**, 1654–1659 (2008).

[7] Muller, D. J., Helenius, J., Alsteens, D. & Dufrene, Y. F. Force probing surfaces of living cells to molecular resolution. *Nat. Chem. Biol.* **5**, 383–390 (2009).

[8] Oesterhelt, F., Oesterhelt, D., Pfeiffer, M., Engel, A., Gaub, H. E. & Muller, D. J. Unfolding pathways of individual bacteriorhodopsins. *Science* **288**, 143–146 (2000).

[9] Scheuring, S. & Sturgis, J. N. Chromatic adaptation of photosynthetic membranes. *Science* **309**, 484–487 (2005).

[10] Stewart, M. P., Helenius, J., Toyoda, Y., Ramanathan, S. P., Muller, D. J. & Hyman, A. A. Hydrostatic pressure and the actomyosin cortex drive mitotic cell rounding. *Nature* **469**, 226–230 (2011).

[11] Williams, P. M., Fowler, S. B., Best, R. B., Toca-Herrera, J. L., Scott, K. A., Steward, A., *et al.* Hidden complexity in the mechanical properties of titin. *Nature* **422**, 446–449 (2003).

[12] Ando, T., Kodera, N., Takai, E., Maruyama, D., Saito, K. & Toda, A. A high-speed atomic force microscope for studying biological macromolecules. *Proc. Natl. Acad. Sci. USA* **98**, 12468–12472 (2001).

[13] Ando, T., Uchihashi, T. & Fukuma, T. High-speed atomic force microscopy for nano-visualization of dynamic biomolecular processes. *Prog. Surf. Sci.* **83**, 337–437 (2008).

[14] Shibata, M., Uchihashi, T., Yamashita, H., Kandori, H. & Ando, T. Structural changes in bacteriorhodopsin in response to alternate illumination observed by high-speed atomic force microscopy. *Angew. Chem. Int. Ed.* **50**, 4410–4413 (2011).

[15] Shibata, M., Yamashita, H., Uchihashi, T., Kandori, H. & Ando, T. High-speed atomic force microscopy shows dynamic molecular processes in photoactivated bacteriorhodopsin. *Nat. Nanotech.* **5**, 208–212 (2010).

[16] Yamashita, H., Inoue, K., Shibata, M., Uchihashi, T., Sasaki, J., Kandori, H., *et al.* Role of trimer-trimer interaction of bacteriorhodopsin studied by optical spectroscopy and high-speed atomic force microscopy. *J. Struct. Biol.* **184**, 2–11 (2013).

[17] Kodera, N., Yamamoto, D., Ishikawa, R. & Ando, T. Video imaging of walking myosin V by high-speed atomic force microscopy. *Nature* **468**, 72–76 (2010).

[18] Uchihashi, T., Iino, R., Ando, T. & Noji, H. High-speed atomic force microscopy reveals rotary catalysis of rotorless F_1-ATPase. *Science* **333**, 755–758 (2011).

[19] Miyagi, A., Chipot, C., Rangl, M. & Scheuring, S. High-speed atomic force microscopy shows that annexin V stabilizes membranes on the second timescale. *Nat. Nanotech.* **11**, 783–790 (2016).

[20] Chiaruttini, N., Redondo-Morata, L., Colom, A., Humbert, F., Lenz, M., Scheuring, S., *et al.* Relaxation of Loaded ESCRT-III Spiral Springs Drives Membrane Deformation. *Cell* **163**, 866–879 (2015).

[21] Crampton, N., Yokokawa, M., Dryden, D. T., Edwardson, J. M., Rao, D. N., Takeyasu, K., *et al.* Fast-scan atomic force microscopy reveals that the type III restriction enzyme EcoP15I is capable of DNA translocation and looping. *Proc. Natl. Acad. Sci. USA* **104**, 12755–12760 (2007).

[22] Miyagi, A., Ando, T. & Lyubchenko, Y. L. Dynamics of nucleosomes assessed with time-lapse high-speed atomic force microscopy. *Biochemistry* **50**, 7901–7908 (2011).

[23] Suzuki, Y., Higuchi, Y., Hizume, K., Yokokawa, M., Yoshimura, S. H., Yoshikawa, K., *et al.* Molecular dynamics of DNA and nucleosomes in solution studied by fast-scanning atomic force microscopy. *Ultramicroscopy* **110**, 682–688 (2010).

[24] Endo, M., Katsuda, Y., Hidaka, K. & Sugiyama, H. Regulation of DNA methylation using different tensions of double strands constructed in a defined DNA nanostructure. *J. Am. Chem. Soc.* **132**, 1592–1597 (2010).

[25] Endo, M., Yang, Y., Suzuki, Y., Hidaka, K. & Sugiyama, H. Single-molecule visualization of the hybridization and dissociation of photoresponsive oligonucleotides and their reversible switching behavior in a DNA nanostructure. *Angew. Chem. Int. Ed.* **51**, 10518–10522 (2012).

[26] Raz, M. H., Hidaka, K., Sturla, S. J., Sugiyama, H. & Endo, M. Torsional Constraints of DNA Substrates Impact Cas9 Cleavage. *J. Am. Chem. Soc.* **138**, 13842–13845 (2016).

[27] Sannohe, Y., Endo, M., Katsuda, Y., Hidaka, K. & Sugiyama, H. Visualization of dynamic conformational switching of the G-quadruplex in a DNA nanostructure. *J. Am. Chem. Soc.* **132**, 16311–16313 (2010).

[28] Mohamed, M. S., Kobayashi, A., Taoka, A., Watanabe-Nakayama, T., Kikuchi, Y., Hazawa, M., *et al.* High-Speed Atomic Force Microscopy Reveals Loss of Nuclear Pore Resilience as a Dying Code in Colorectal Cancer Cells. *ACS Nano* **11**, 5567–5578 (2017).

[29] Sakiyama, Y., Mazur, A., Kapinos, L. E. & Lim, R. Y. Spatiotemporal dynamics of the nuclear pore complex transport barrier resolved by high-speed atomic force microscopy. *Nat. Nanotech.* **11**, 719–723 (2016).

[30] Shibata, M., Uchihashi, T., Ando, T. & Yasuda, R. Long-tip high-speed atomic force microscopy for nanometer-scale imaging in live cells. *Sci. Rep.* **5**, 8724 (2015).

[31] Watanabe, H., Uchihashi, T., Kobashi, T., Shibata, M., Nishiyama, J., Yasuda, R., *et al.* Wide-area scanner for high-speed atomic force microscopy. *Rev. Sci. Instrum.* **84**, 053702 (2013).

[32] Uchihashi, T., Watanabe, H., Fukuda, S., Shibata, M. & Ando, T. Functional extension of high-speed AFM for wider biological applications. *Ultramicroscopy* **160**, 182–196 (2016).

[33] Uchihashi, T., Kodera, N. & Ando, T. Guide to video recording of structure dynamics and dynamic processes of proteins by high-speed atomic force microscopy. *Nat. Protoc.* **7**, 1193–1206 (2012).

[34] Casella, J. F., Flanagan, M. D. & Lin, S. Cytochalasin D inhibits actin polymerization and induces depolymerization of actin filaments formed during platelet shape change. *Nature* **293**, 302–305 (1981).

[35] Beaudoin, G. M. 3rd, Lee, S. H., Singh, D., Yuan, Y., Ng, Y. G., Reichardt, L. F., *et al.* Culturing pyramidal neurons from the early postnatal mouse hippocampus and cortex. *Nat. Protoc.* **7**, 1741–1754 (2012).

[36] de Lima, A. D., Merten, M. D. & Voigt, T. Neuritic differentiation and synaptogenesis in serum-free neuronal cultures of the rat cerebral cortex. *J. Comp. Neurol.* **382**, 230–246 (1997).

[37] Fath, T., Ke, Y. D., Gunning, P., Gotz, J. & Ittner, L. M. Primary support cultures of hippocampal and substantia nigra neurons. *Nat. Protoc.* **4**, 78–85 (2008).

[38] Kaech, S. & Banker, G. Culturing hippocampal neurons. *Nat. Protoc.* **1**, 2406–2415 (2006).

[39] Chacko, J. V., Zanacchi, F. C. & Diaspro, A. Probing cytoskeletal structures by coupling optical superresolution and AFM techniques for a correlative approach. *Cytoskeleton (Hoboken)* **70**, 729–740 (2013).

[40] Hell, S. W. Far-field optical nanoscopy. *Science* **316**, 1153–1158 (2007).